Biochemistry

 Volume 36, Number 19 May 13, 1997

Accelerated Publications

Potent Bifunctional Anticoagulants: Kunitz Domain−Tissue Factor Fusion Proteins

Geoffrey F. Lee, Robert A. Lazarus, and Robert F. Kelley*

Department of Protein Engineering, Genentech, Inc., 460 Point San Bruno Boulevard, South San Francisco, California 94080

Received February 20, 1997[⊗]

ABSTRACT: A strategy to design potent antagonists of human coagulation factor VIIa (FVIIa) by linking two proteins that independently inhibit activity and bind at separate, nonoverlapping sites is presented. A bifunctional inhibitor (KDTF5), comprising a Kunitz-type domain engineered to inhibit the FVIIa active site and a soluble tissue factor (TF) variant that is defective as a cofactor for factor X (FX) activation, was developed from structure-based modeling of a ternary FVIIa−Kunitz domain−TF complex. KDTF5 inhibited FVIIa-dependent FX activation with a K_i* of 235 ± 45 pM, a 193-fold and 398-fold increase in potency compared to the TF variant and Kunitz domain individually. Similarly, KDTF5 was a more potent anticoagulant *in vitro* compared to either inhibitory domain alone. The results demonstrate the harnessing of a macromolecular chelate effect by fusing two inhibitory ligands that bind a target at spatially distinct sites.

Factor VIIa (FVIIa)[1] in complex with its obligate, membrane-bound cofactor, tissue factor (TF), triggers vertebrate blood coagulation (*1*−*3*). TF·FVIIa-mediated activation of factor X (FX) to factor Xa (FXa), and of factor IX to factor IXa, leads to thrombin production and ultimately to formation of fibrin clots at sites of vascular injury. Pathological consequences of TF·FVIIa-initiated clotting include deep vein thrombosis following trauma or surgery and disseminated intravascular coagulation associated with septicemia (*4*). In addition, TF·FVIIa-mediated thrombosis has been implicated in the episodic progression of atherosclerotic diseases (*5*). Potent and selective inhibitors of TF·FVIIa would thus further our understanding of the role of this complex as an initiator of coagulation and aid in evaluating FVIIa as a target in the development of anticoagulants for thrombotic disorders.

Our laboratories have previously characterized two proteins that block TF•FVIIa-triggered coagulation by binding to FVIIa. One was hTFAA, the soluble extracellular domain of human TF containing alanine substitutions for lysines at residues 165 and 166 (*6*−*8*). hTFAA is defective as a cofactor for FX activation but competes with wild-type TF for binding to FVIIa (*9*) and is a potent and FVIIa-selective antithrombotic agent (*10*). The other was the Kunitz-type protease inhibitor domain TF7I-C, which had been engineered by monovalent phage display to potently bind the protease active site of FVIIa (*11*). The recently solved crystal structure of TF·FVIIa (*12*) showed the TF and protease inhibitor binding sites to be spatially distinct. We thus explored the possibility of linking the two inhibitors as a means of creating a bifunctional fusion protein with dramatically enhanced affinity for the coagulation factor compared to that of either fusion partner alone. Here, we report on the design, production, and testing of Kunitz domain−tissue factor (KDTF) fusion proteins that potently inhibit FVIIa-

* Corresponding author. Phone: (415) 225-2321. Fax: (415) 225-3734. E-mail: rk@gene.com.

⊗ Abstract published in *Advance ACS Abstracts,* April 15, 1997.

[1] Abbreviations: FVIIa, human coagulation factor VIIa; FX and FXa, human coagulation factors X and Xa, respectively; TF, tissue factor; hTFAA, the soluble extracellular domain of TF, residues 1−219, containing lysine to alanine substitutions at positions 165 and 166; APPI, Alzheimer's amyloid β-protein precursor inhibitor; KDTF, Kunitz domain−tissue factor fusion protein; TFPI-KD1, the first Kunitz domain of the tissue factor pathway inhibitor; PT, prothrombin time.

S0006-2960(97)00388-7 CCC: $14.00

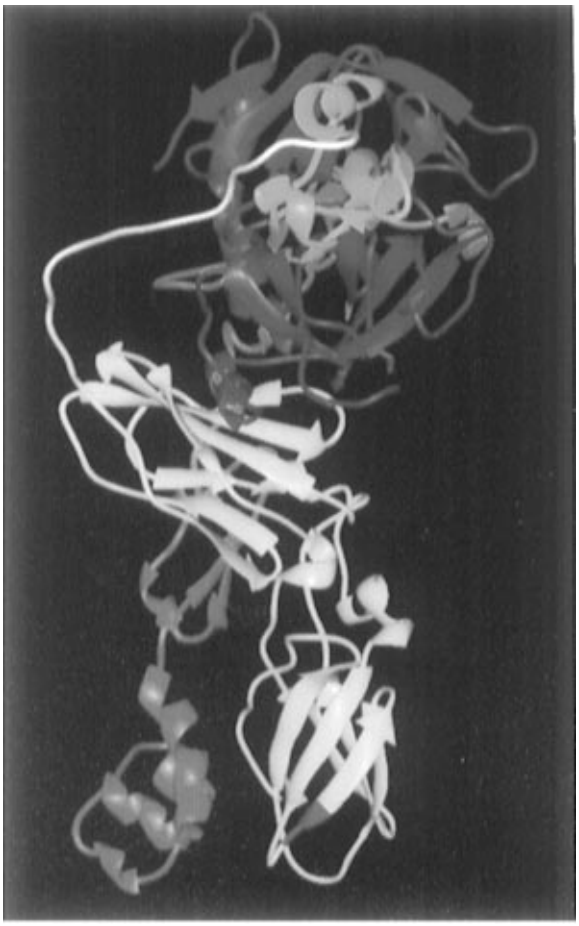

FIGURE 1: Ribbon diagram model of KDTF binding to factor VIIa. The soluble extracellular domain of tissue factor (in yellow) binding to FVIIa (light chain in green, protease domain in red) is based on a 2.0 Å resolution structure of the complex (*12*). The position of alanine substitutions in hTFAA is indicated in magenta. Kunitz domain TF7I-C (in blue) binding to the active site of FVIIa was modeled using the coordinates of APPI binding to trypsin, a related protease−inhibitor complex whose structure was determined at 1.8 Å resolution. A 22-residue linker, in extended conformation (in white), was used to connect the COOH terminus of the Kunitz domain to the NH_2 terminus of TF. The distance between these termini is ≈60 Å.

mediated proteolysis by harnessing a macromolecular chelate effect.

EXPERIMENTAL PROCEDURES

Molecular Modeling. Kunitz domain binding to the TF·FVIIa active site was based on Alzheimer's amyloid β-protein precursor inhibitor (APPI) binding to trypsin (T. R. Hynes, A. A. Kossiakoff, and J. A. Wells, unpublished results) and was modeled by alignment of conserved catalytic triad residues from each crystal structure using MidasPlus (*13*). The model included a 22-residue linker, with residues in extended conformation, to span the ≈60 Å distance between the COOH terminus of the Kunitz domain and the NH_2 terminus of TF.

Gene Construction. The gene encoding a Kunitz domain−tissue factor fusion protein containing a single -$(Gly)_4$-Ser-(G_4S) linker module between domains (termed KDTF1) was made by directional cloning of a DNA fragment encoding TF7I-C (*11*) and an oligonucleotide cassette encoding the G_4S linker into a phagemid vector encoding hTFAA (*9*) using standard molecular biology techniques (*14*). Unique restriction sites flanking the G_4S-encoding cassette allowed insertion of other oligonucleotide cassettes designed to encode the linker modules in KDTF2−KDTF7. Dideoxynucleotide sequencing (*15*) was used to confirm correct linker construction.

Fusion Protein Purification. TF-containing proteins were expressed by secretion from *Escherichia coli* and purified by immunoaffinity chromatography as previously described (*9*). In some cases, a final size-exclusion chromatography step, using a Superdex 75 column equilibrated in phosphate-buffered saline, was incorporated to purify KDTF monomers from putative oligomers. Coomassie blue-stained 4−20% SDS−PA gels indicated each purified KDTF preparation was ≥95% homogeneous. Mass analysis of purified samples was performed on a Sciex API III mass spectrometer equipped with an articulated electrospray source.

Concentration Determinations. Selected KDTF preparations were assayed for tissue factor concentration on the basis of initial rates of binding to monoclonal antibody D3 using a Pharmacia BIAcore instrument. The D3 antibody was immobilized through amine coupling, and binding rates were determined under mass transfer-limiting conditions as previously described (*16*). Initial rates of hTFAA binding under these conditions were directly proportional to hTFAA concentration in the range of 1 nM−1 μM. The rate vs concentration relationship was used to construct standard curves from which fusion protein apparent TF domain concentrations could be calculated on the basis of initial rates of KDTF binding. Since BIAcore-measured resonance units are directly proportional to the mass of the ligands being bound, multiplication of the apparent TF domain concentration by the ratio of the molecular weight of hTFAA to that of the KDTF in question produced a corrected TF domain concentration. Kunitz domain concentrations of the same preparations were determined by trypsin active site titration (*11*), using known concentrations of ecotin as inhibitor standard. Concentration of total protein was obtained from spectrophotometric measurements at 280 nm (*17*).

Factor X Activation Assay. Conversion of zymogen to activated factor X by TF·FVIIa was measured in a two-stage chromogenic assay. Inhibitor was equilibrated at 37 °C with 100 pM FVIIa and 200 nM FX (both factors were from Haematologic Technologies) in 20 mM HEPES, 150 mM NaCl, 5 mM $CaCl_2$, and 0.1% PEG-8000, pH 7.2. FX activation was initiated by adding a transmembrane form of TF (residues 1−243), reconstituted into 70% phosphatidylcholine:30% phosphatidylserine-containing vesicles (*18*), to a concentration of 100 pM. At intervals after TF addition, samples of the reaction mixture were quenched with an equal volume of 50 mM EDTA, pH 8, and then assayed for FXa activity in the buffer above, containing 25 mM EDTA instead of $CaCl_2$, by adding Spectrozyme−FXa (American Diagnostica) to 0.5 mM concentration. Reactions performed as above, but in the absence of inhibitor or in the absence of FX, were used to define uninhibited and background proteolytic rates, respectively. Substrate cleavage rates were converted to moles of FXa produced via standard curves prepared using purified FXa (Haematologic Technologies). Rates of FX activation were determined by linear regression analysis from plots of the moles of FXa produced over the assay time course.

Apparent Equilibrium Inhibition Constant (K_i) Determination.* K_i^* values were calculated using rates of FX

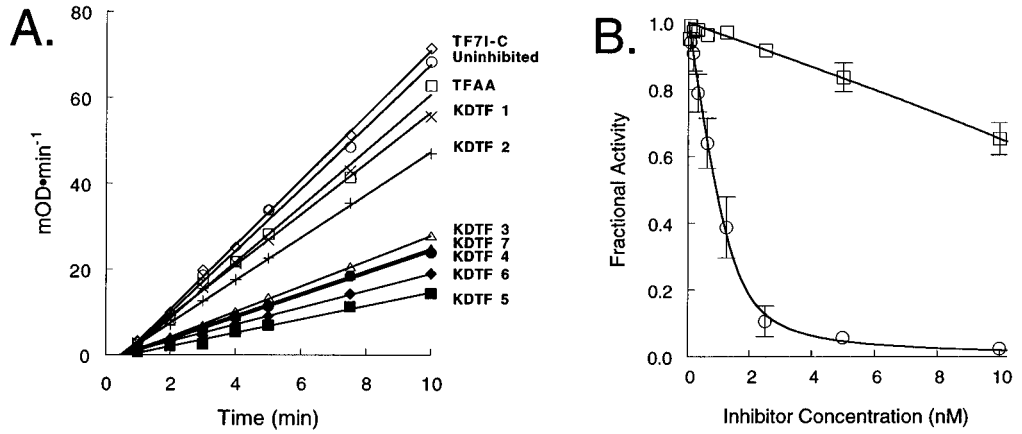

FIGURE 2: KDTF inhibition of FVIIa. (A) Inhibition as a function of linker length. The rate of FXa cleavage of chromogenic substrate (in mOD·min^{-1}) was used to gauge the ability of KDTF proteins, as well as hTFAA and TF7I-C, to inhibit FVIIa-dependent FX activation. The proteins tested, and their rank order of potency (from low to high), are shown from top to bottom in the right margin of the panel. (B) K_i* determination for inhibition of FX activation by KDTF5 (circles) and by an equimolar mixture of TF7I-C and hTFAA (squares). The mixture concentration was defined in terms of KDTF5 equivalents, where 1 mol of KDTF5 equals 1 mol each of hTFAA and TF7I-C. The data are averages of three independent experiments with each inhibitory sample; standard errors are indicated by bars for those points for which values exceed symbol size. The lines represent nonlinear regression fits to the data using an equation derived for tight-binding inhibitors (see Experimental Procedures).

activation obtained over ranges of inhibitor concentration by fitting the activity vs concentration data via nonlinear regression to an equation derived for tight-binding inhibitors:

$$V_i/V_0 = 1 - \frac{[E_0] + [I_0] + K_i^* - \sqrt{([E_0] + [I_0] + K_i^*)^2 - (4[E_0][I_0])}}{2[E_0]}$$

where V_i/V_0 is fractional activity (the steady-state inhibited rate divided by the uninhibited rate), $[E_0]$ is the total TF/FVIIa concentration, and $[I_0]$ is the total inhibitor concentration (*19*, *20*).

Prothrombin Time Clotting Assay. Prothrombin time (PT) assays were performed in an ACL 300 coagulometer, operated in research mode, by mixing 25 mM $CaCl_2$ containing inhibitor and 500 pM FVIIa, preequilibrated for 1 h at room temperature, with an equal volume of citrated FVII-deficient human plasma (George King BioMedical) containing 500 pM relipidated TF(1−243).

RESULTS

Inhibitor Design. Molecular modeling of Kunitz domain binding into the active site of TF·FVIIa suggested that connecting the COOH terminus of TF7I-C to the NH_2 terminus of hTFAA via a flexible polypeptide linker would create a bifunctional fusion protein whose inhibitory domains could bind a single FVIIa without steric restraints (Figure 1). The model, however, had limited utility for determining an optimal linker length since the last two COOH-terminal residues of the Kunitz domain and the five most NH_2-terminal residues of TF were disordered in their respective structures. Also, the N-linked oligosaccharide chain protruding from Asn-322 of the FVIIa protease domain (*21*), a potential obstacle lying in the vicinity of the shortest linker path between inhibitory domains, was not observed in the TF·FVIIa structure. In light of these limitations, the linker between domains was designed in a modular format, with each module containing a -$(Gly)_4$-Ser- (G_4S) sequence. We therefore created a series of genes encoding an NH_2-terminal TF7I-C, a COOH-terminal hTFAA, and from 1 to 7 linker modules between the inhibitory domains; the Kunitz domain-tissue factor fusion proteins were designated KDTF1 to KDTF7, respectively.

Table 1: Structural Integrity of Purified Fusion Proteins

protein	tissue factor concn[a] (μM)	Kunitz domain concn[a] (μM)	total protein concn[a] (μM)
KDTF1	72	77	76
KDTF2	65	64	66
KDTF3	36	38	36
KDTF4	36	35	31
KDTF5	19	17	16
KDTF6	29	25	39
KDTF7	33	30	47

[a] Concentration determinations were based on binding to monoclonal antibody D3 (for hTFAA), on trypsin active site titration (for TF7I-C), and on absorbance at 280 nm (for total protein), as described in Experimental Procedures. The estimated standard errors for the TF and Kunitz domain concentration determinations are ±4% and ±11%, respectively.

Expression of Properly Folded Fusion Proteins. We purified the fusion proteins from periplasmic shockates and then tested selected preparations to verify that each product was properly folded. Mass spectrometry revealed that each purified KDTF had a mass corresponding to the desired product containing five disulfide bonds (data not shown). In order to establish that each KDTF contained an intact TF and Kunitz domain moiety, selected preparations were assayed for the ability to bind monoclonal antibody D3, which recognizes a nonlinear epitope in the carboxy-terminal extracellular domain of TF (*22*), and for the ability to inhibit trypsin. Concentrations of functional domains derived from these analyses were compared to the total protein concentration obtained from spectrophotometric measurements at 280 nm. The results, shown in Table 1, demonstrated that each fusion protein was comprised of a properly folded TF moiety and a functionally active protease inhibitor.

Linker Length Dependence of FVIIa Inhibition. Each KDTF was characterized with respect to its ability to block FVIIa-mediated proteolytic activation of FX. Performed at a constant inhibitor concentration of 1 nM, the FX activation assay indicated that fusion proteins containing fewer than

Table 2: Binding Parameters Determined from (A) FX Activation Assays and (B) Prothrombin Time Assay-Based Scatchard Analyses[a]

	(A) factor X activation assay		(B) prothrombin time assay/Scatchard analysis		
inhibitor	K_i* (nM)	relative potency (%)	K_d (nM)	relative potency (%)	stoichiometry
KDTF5	0.235 ± 0.045	100	0.121 ± 0.029	100	0.97 ± 0.01:1
hTFAA	45.3 ± 7.0	0.52	13.2 ± 4.3	0.92	0.98 ± 0.02:1
TF7I-C	93.6 ± 9.2	0.25	62.3 ± 13.0	0.19	0.99 ± 0.01:1
mixture[b]	3.81 ± 0.52	6.17	0.289 ± 0.056	41.9	0.92 ± 0.02:1

[a] Binding constants and stoichiometries are expressed as mean values ± SEM for two or more independent experiments. [b] Mixture refers to an equimolar combination of TF7I-C and hTFAA. Mixture concentrations are expressed as KDTF5 equivalents, where 1 mol of KDTF5 = 1 mol each of TF7I-C and hTFAA.

three G_4S modules, as well as TF7I-C and hTFAA alone, were considerably less potent than those containing three or more spacer units (Figure 2A). This observation was consistent with the molecular model (Figure 1), which suggested that linkers containing less than three G_4S modules would be too short to allow efficient binding of both inhibitory domains to a single FVIIa target. For the KDTF proteins with three or more linker modules, potency increased in the series from KDTF3 to KDTF5 and then decreased in the series from KDTF5 to KDTF7. Thus KDTF5, containing a 25-residue linker, proved to be the optimal construct in this series for FVIIa inhibition.

Potency of FVIIa Inhibition. The FX activation assay was also used to determine apparent equilibrium inhibition constants (K_i*) for KDTF5, for hTFAA and TF7I-C individually, and for an equimolar mixture of hTFAA and TF7I-C. When FX activation was assayed over a range of inhibitor concentrations, a K_i* value of 235 pM was calculated for KDTF5 binding to FVIIa (Figure 2B). Significantly, KDTF5 was 193- and 398-fold more potent than hTFAA and TF7I-C, respectively, and greater than 16-fold more potent than an equimolar combination of the two separate inhibitors (Figure 2B and Table 2A). In order to independently corroborate the affinity measurements derived from the FX activation assay, a prothrombin time (PT) based coagulation assay was developed from which Scatchard analysis could be performed. Initial PT assays, performed in the absence of inhibitor and with varying FVIIa concentrations, indicated clotting times were directly proportional to the logarithm of the FVIIa concentration, in the range of 7.8−250 pM. This relationship allowed us to estimate levels of free FVIIa in PT experiments performed at a fixed total concentration of FVIIa and in the presence of varied concentrations of inhibitor. Levels of free and bound inhibitor deduced from free FVIIa concentrations were then used for Scatchard analysis (*23*). When KDTF5 was tested in this manner, the analysis indicated that our optimal fusion protein has a K_d of 121 pM for FVIIa and binds with 1:1 stoichiometry (Figure 3). Results for similar analyses of hTFAA and TF7I-C, and for the equimolar combination of inhibitors, are summarized in Table 2B. Although KDTF5 was more potent than the equimolar combination of inhibitors in both assays, the mixture of inhibitors was considerably more potent than either inhibitor alone. We attribute this phenomenon in large part to the observation that TF7I-C has a 7-fold higher affinity for the TF·FVIIa complex relative to FVIIa alone (*11*). We also noted that the noncovalent mixture of inhibitors was considerably more potent in the PT, compared to the FX activation, assay. This may be due to the inhibition of other coagulation factors present in plasma and absent from the activation assay, which would contribute to prolonged clot times and thus an apparent increase in potency. In particular, Kunitz domain TF7I-C is known to potently inhibit factor XIa and plasma kallikrein and to prolong clotting triggered by both the intrinsic and extrinsic coagulation cascades, in *in vitro* assays (*11*).

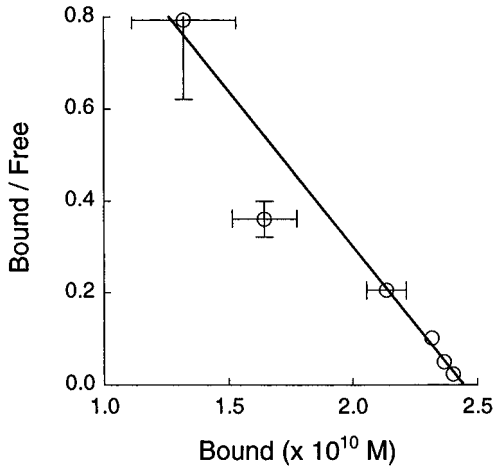

FIGURE 3: Prothrombin time (PT) assay-based Scatchard analysis. Scatchard plot of KDTF5 binding to FVIIa. The data are averages for four independent experiments; bars indicate standard errors for those points for which values exceed the symbol size.

DISCUSSION

Putative Mechanism of Anticoagulant Function. We have engineered a novel high-affinity FVIIa antagonist by fusing two inhibitory proteins that bind the target at spatially distinct sites. The demonstration of KDTF linker length dependence for FVIIa inhibition and of the 1:1 stoichiometry of binding calculated from Scatchard analysis strongly suggests that KDTF5 functions by chelating a single FVIIa molecule, rather than by cross-linking to form $(KDTF5{\cdot}FVIIa)_n$ oligomers. Unlike previous efforts to generate a bifunctional TF·FVIIa inhibitor (*24*), by linking the first Kunitz domain of tissue factor pathway inhibitor (TFPI-KD1) to the light chain of FX, the KDTF construct presented here has the advantage that both inhibitory components are known to bind FVIIa, and not TF, allowing us to specifically analyze the contributions of each fusion partner to the overall affinity for FVIIa inhibition.

Additionally, both the FX activation and prothrombin time assays were performed by equilibration of KDTF5 with FVIIa and then initiating reactions by adding relipidated TF. Since one KDTF fusion partner is a TF variant that binds FVIIa with wild-type soluble TF affinity, potent inhibition of FVIIa using this assay format suggests that KDTF5 is capable of directly inhibiting FVIIa, free from the requirement of the coagulation factor forming a complex with cell surface TF. This mode of action is distinctly different from

that of other potent FVIIa inhibitors, including the FX_{LC}·TFPI-KD1 hybrid (*24*), TFPI itself (*25*), and the hookworm anticoagulant AcAPc2 (*26*), each of which inhibits only in the context of TF·FVIIa or TF·FVIIa·FX complexes on membrane surfaces. As far as we are aware, KDTF5 is thus the most potent direct FVIIa inhibitor described to date.

Harnessing a Chelate Effect. In principle, the bifunctional inhibitor would be expected to have an affinity approaching the product of those of the individual components divided by the local effective concentration of the unbound inhibitory domain once one domain has bound FVIIa (*27*, *28*). The incorporation of a flexible linker to connect the KDTF inhibitory domains, therefore, is a suboptimal design for maximizing affinity. Making the linker more rigid or building in linker−target interactions are two potential approaches for generating an even higher affinity bifunctional inhibitor. Alternatively, potency could be enhanced by incorporating the transmembrane domain of TF into KDTF5 and reconstituting this variant into phospholipid vesicles. Since FVIIa affinity for relipidated TF is about 1000-fold higher than its affinity for soluble TF (*29*), such a variant could harness an additional chelate effect through the interaction of the FVIIa γ-carboxyglutamic acid-containing (Gla) domain with the phospholipid surface.

Strikingly, some naturally occurring proteins have also apparently taken advantage of the bifunctional inhibitor strategy to evolve as anticoagulants. Notably, hirudin (*30*) and rhodniin (*31*) are potent bifunctional thrombin inhibitors composed of linked domains, one of which binds and blocks the active site while the other occupies the anion-binding exosite. Analysis of the separate hirudin domains (*32*) demonstrated that the inhibitory potential of the intact molecule approaches that of the product of the fragments' affinities, suggesting that nature has likewise harnessed this powerful strategy to evolve potent antagonists of protein−protein interactions.

ACKNOWLEDGMENT

We thank Han Chen and Brad Snedecor for production of cell pastes containing fusion proteins, Beth Gillece-Castro and Jim Bourell for mass analyses, Mark Vasser and Parkash Jhurani for oligonucleotide synthesis, and Mark Dennis for helpful discussions on performing the trypsin inhibition assay. In addition, we thank David Banner (Hoffmann-La Roche) for the TF·FVIIa crystal structure coordinates and Yves Muller, Axel Scheidig, and Charlie Eigenbrot for help in developing the model shown in Figure 1.

REFERENCES

1. Nemerson, Y. (1988) *Blood 71*, 1.
2. Davie, E. W. (1995) *Thromb. Haemostasis 74*, 1.
3. Rapaport, S. I., and Rao, L. V. M. (1995) *Thromb. Haemostasis 74*, 7.
4. Broze, G. J., Jr. (1994) in *Haemostasis and Thrombosis* (Bloom, A. L., Forbes, C. D., Thomas, D. P., and Tuddenham, E. G. D., Eds.) pp 349−377, Churchill Livingstone, Edinburgh.
5. Wilcox, J. N., and Harker, L. A. (1994) in *Haemostasis and Thrombosis* (Bloom, A. L., Forbes, C. D., Thomas, D. P., and Tuddenham, E. G. D., Eds.) pp 1139−1152, Churchill Livingstone, Edinburgh.
6. Roy, S., Hass, P. E., Bourell, J. H., Henzel, W. J., and Vehar, G. A. (1991) *J. Biol. Chem. 266*, 22063.
7. Ruf, W., Miles, D. J., Rehemtulla, A., and Edgington, T. S. (1992) *J. Biol. Chem. 267*, 6375.
8. Ruf, W., Miles, D. J., Rehemtulla, A., and Edgington, T. S. (1992) *J. Biol. Chem. 267*, 22206.
9. Kelley, R. F., Costas, K. E., O'Connell, M. P., and Lazarus, R. A. (1995) *Biochemistry 34*, 10383.
10. Kelley, R. F., O'Connell, M. P., Modi, N., Refino, C. J., Pater, C., and Bunting, S. J. (1997) *Blood 89*, 3219.
11. Dennis, M. S., and Lazarus, R. A. (1994) *J. Biol. Chem. 269*, 22129.
12. Banner, D. W., D'Arcy, A., Chène, C., Winkler, F. K., Guha, A., Konigsberg, W. H., Nemerson, Y., and Kirchhofer, D. (1996) *Nature 380*, 41.
13. Ferrin, T. E., Huang, C. C., Jarvis, L. E., and Langridge, R. (1988) *J. Mol. Graphics 6*, 13.
14. Sambrook, J., Fritsch, E. F., and Maniatis, T. (1989) *Molecular Cloning: A Laboratory Manual*, Cold Spring Harbor Laboratory Press, Plainview, NY.
15. Sanger, F., Nicklen, S., and Coulsen, A. R. (1977) *Proc. Natl. Acad. Sci. U.S.A. 74*, 5463.
16. Karlsson, R., Roos, H., Fägerstam, L., and Persson, B. (1994) *Methods: A Companion to Methods in Enzymology*, Vol. 6, p 99, Academic Press, New York.
17. Gill, S. C., and von Hippel, P. H. (1989) *Anal. Biochem. 182*, 319.
18. Bach, R., Gentry, R., and Nemerson, Y. (1986) *Biochemistry 25*, 4007.
19. Bieth, J. (1974) in *Proteinase Inhibitors* (Fritz, H., Tschesche, H., Greene, L. J., and Truscheit, E., Eds.) pp 463−469, Springer-Verlag, New York.
20. Williams, J. W., and Morrison, J. F. (1979) *Methods Enzymol. 63*, 437.
21. Thim, L., Bjoern, S., Christensen, M., Nicolaisen, E. M., Lund-Hansen, T., Pedersen, A. H., and Hedner, U. (1988) *Biochemistry 27*, 7785.
22. Paborsky, L. R., Tate, K. M., Harris, R. J., Yansura, D. G., Band, L., McCray, G., Gorman, C. M., O'Brien, D. P., Chang, J. Y., Swartz, J. R., Fung, V. P., Thomas, J. N., and Vehar, G. A. (1989) *Biochemistry 28*, 8072.
23. Dahlquist, F. W. (1978) *Methods Enzymol. 48*, 270.
24. Girard, T. J., MacPhail, L. A., Likert, K. M., Novotny, W. F., Miletich, J. P., and Broze, G. J., Jr. (1990) *Science 248*, 1421.
25. Broze, G. J., Jr., Warren, L. A., Novotny, W. F., Higuchi, D. A., Girard, T. J., and Miletich, J. P. (1988) *Blood 71*, 335.
26. Stanssens, P., Bergum, P. W., Gansemans, Y., Jespers, L., Laroche, Y., Huang, S., Maki, S., Messens, J., Lauwereys, M., Cappello, M., Hotez, P. J., Lasters, I., and Vlasuk, G. P. (1996) *Proc. Natl. Acad. Sci. U.S.A. 93*, 2149.
27. Jencks, W. P. (1981) *Proc. Natl. Acad. Sci. U.S.A. 78*, 4046.
28. Creighton, T. E. (1984) in *Proteins*, pp 360−365, W. H. Freeman and Co., New York.
29. Waxman, E., Ross, J. B. A., Laue, T. M., Guha, A., Thiruvikraman, S. V., Lin, T.C., Konigsberg, W. H., and Nemerson, Y. (1992) *Biochemistry 31*, 3998.
30. Rydel, T. J., Ravichandran, K. G., Tulinsky, A., Bode, W., Huber, R., Roitsch, C., and Fenton, J. W., Jr. (1990) *Science 249*, 277.
31. van de Locht, A., Lamba, D., Bauer, M., Huber, R., Friedrich, T., Kröger, B., Höffken, W., and Bode, W. (1995) *EMBO J. 14*, 5149.
32. Dennis, S., Wallace, A., Hofsteenge, J., and Stone, S. R. (1990) *Eur. J. Biochem. 188*, 61.

BI970388J